Check for updates

ChemSusChem

Chemistry–Sustainability–Energy–Materials

Chemistry Europe

European Chemical Societies Publishing

Accepted Article

Title: Optimized Incorporation of Furan into Diketopyrrolopyrrole-Based Conjugated Polymers for Organic Field-Effect Transistors

Authors: Justin Neu, Kan Ding, Shubin Liu, Harald Ade, Jie Xu, and Wei You

This manuscript has been accepted after peer review and appears as an Accepted Article online prior to editing, proofing, and formal publication of the final Version of Record (VoR). The VoR will be published online in Early View as soon as possible and may be different to this Accepted Article as a result of editing. Readers should obtain the VoR from the journal website shown below when it is published to ensure accuracy of information. The authors are responsible for the content of this Accepted Article.

To be cited as: *ChemSusChem* **2024**, e202400171

Link to VoR: https://doi.org/10.1002/cssc.202400171

WILEY VCH

10.1002/cssc.202400171

Optimized Incorporation of Furan into Diketopyrrolopyrrole-Based Conjugated Polymers for Organic Field-Effect Transistors

Justin Neu,[a] Kan Ding,[c] Shubin Liu,[d] Harald Ade,[c] Jie Xu,*[b] and Wei You*[a]

[a]Department of Chemistry, University of North Carolina at Chapel Hill, Chapel Hill, North Carolina 27599, USA

[b]Nanoscience and Technology Division, Argonne National Laboratory, Lemont, Illinois 60439, USA

[c]Department of Physics and ORaCEL, North Carolina State University, Raleigh, North Carolina 27695, USA

[d]Research Computing Center, University of North Carolina at Chapel Hill, Chapel Hill, North Carolina 27599, USA

*Email: wyou@unc.edu

Table of Contents:

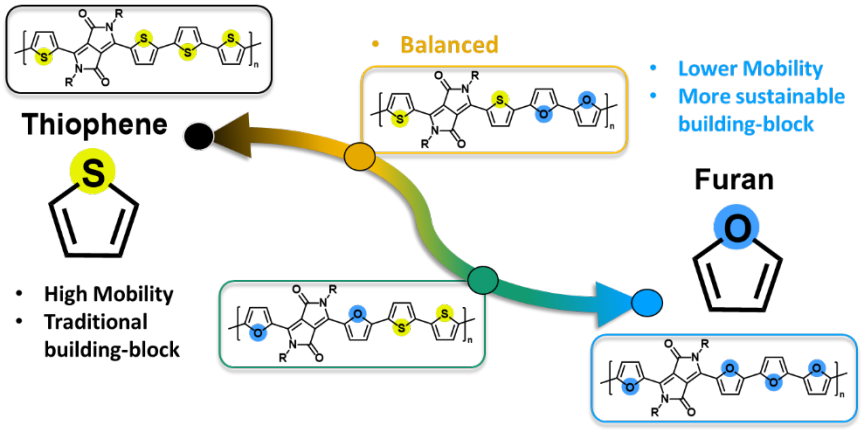

TOC Text Suggestion: To promote sustainability, we selectively introduced furan into the conjugated backbone of a high-mobility polymer scaffold and systematically studied the effect on the microstructure and charge transport. We show that partially and selectively replacing thiophene units with furan can yield nearly comparable performance compared to the all-thiophene polymer.

Key Words: Organic field-effect transistors, Conjugated polymers, Sustainable polymers, Furan, High-mobility.

This article is protected by copyright. All rights reserved.

Accepted Manuscript

1864564x, ja, Downloaded from https://chemistry-europe.onlinelibrary.wiley.com/doi/10.1002/cssc.202400171 by Argonne National Laboratory, Wiley Online Library on [25/03/2024]. See the Terms and Conditions (https://onlinelibrary.wiley.com/terms-and-conditions) on Wiley Online Library for rules of use; OA articles are governed by the applicable Creative Commons License

1864564x, ja, Downloaded from https://chemistry-europe.onlinelibrary.wiley.com/doi/10.1002/cssc.202400171 by Argonne National Laboratory, Wiley Online Library on [25/03/2024]. See the Terms and Conditions (https://onlinelibrary.wiley.com/terms-and-conditions) on Wiley Online Library for rules of use; OA articles are governed by the applicable Creative Commons License

Accepted Manuscript

ABSTRACT

Flexible electronics have received considerable attention in the past decades due to their promising application in rollable display screens, wearable devices, implantable devices, and other electronic applications. In particular, conjugated polymers are favored for flexible electronics due to their mechanical flexibility and potential for solution-processed fabrication techniques, such as blade-coating, roll-to-roll printing, and high-throughput printing allowing for high-performance transistor devices. Thiophene is the prevailing conjugated unit to construct these conjugated polymers due to its favorable electronic properties. On the other hand, furans are among the few conjugated moieties that are easily derived from bio renewable resources. To promote sustainability, we selectively introduced furan into the conjugated backbone of a high-mobility polymer scaffold and systematically studied the effect on the microstructure and charge transport. We show that partially and selectively replacing thiophene units with furan can yield nearly comparable performance compared to the all-thiophene polymer. This strategy offers an improvement in the sustainability of the polymer by incorporating bio-sourced furan without sacrificing the high-performance characteristics. Meanwhile, polymers with incorrect or complete furan incorporation show reduced mobilities. This work serves to develop coherent structure–morphology–performance relationships; such knowledge will establish guidelines for the future development of sustainable, furan-based conjugated materials.

This article is protected by copyright. All rights reserved.

1864564x, ja, Downloaded from https://chemistry-europe.onlinelibrary.wiley.com/doi/10.1002/cssc.202400171 by Argonne National Laboratory, Wiley Online Library on [25/03/2024]. See the Terms and Conditions (https://onlinelibrary.wiley.com/terms-and-conditions) on Wiley Online Library for rules of use; OA articles are governed by the applicable Creative Commons License

Accepted Manuscript

INTRODUCTION

Flexible electronics have received considerable attention in the past decades due to their promising application in rollable display screens, wearable devices, implantable devices, and others.[1,2] Organic field-effect transistors (OFETs) have tremendous potential in flexible electronic devices due to the ability to process these materials at large-scale from solution. In particular, conjugated polymers are favored due to their mechanical flexibility and potential for solution-processed fabrication techniques, such as blade-coating, roll-to-roll printing, and high-throughput printing allowing for high-performance transistor devices.[3–5] Since the first examples of using polythiophenes in OFETs,[6] significant advancements have been made as key device figure of merits have become comparable, or even surpassed those of amorphous silicon;[7,8] for example, charge carrier mobilities over 10 $cm^2\ V^{-1}\ s^{-1}$ have been reported for OFETs based on conjugated polymers.[9–12] The tremendous improvement of the OFETs performance has been driven by advancements in polymer design, processing, and device optimization.

From the perspective of polymer design, most attention has been paid to engineering the molecular structure to achifeve desirable optical, electronic and transport properties for specific applications. These designs have mainly focused on developments of the conjugated backbone or the solubilizing side chains.[13,14] Of the many molecular designs that have been conceived, diketopyrrolopyrrole (DPP)-containing polymers are one of the most common for OFETs.[15,16] The structure-property relationships of DPP-based polymers have been extensively studied and developed from the early examples.[3,17–19] One common feature of all DPP based polymers is the incorporation of chalcogen atoms (e.g., S in the form of thiophene) into conjugated materials due to the facile modulation of optoelectronic properties and intra/intermolecular interactions. In fact, thiophene as a structural unit has been employed in almost all high-performance conjugated polymers for optoelectronics (particularly solar cells and OFETs), due to several factors including well-developed synthetic chemistry and good electronic properties.[20–23]

However, the commercial-scale manufacture of thiophene heavily relies on petroleum based raw materials. Typically, the industrial process involves a two-component reaction wherein a 4-carbon chain

This article is protected by copyright. All rights reserved.

1864564x, ja, Downloaded from https://chemistry-europe.onlinelibrary.wiley.com/doi/10.1002/cssc.202400171 by Argonne National Laboratory, Wiley Online Library on [25/03/2024]. See the Terms and Conditions (https://onlinelibrary.wiley.com/terms-and-conditions) on Wiley Online Library for rules of use; OA articles are governed by the applicable Creative Commons License

Accepted Manuscript

molecule reacts with a sulfur source over a catalyst. A range of suitable feedstocks include butane, n-butanol, among others, all of which are petroleum-based chemicals; the sulfur source can include sulfur, hydrogen sulfide, and carbon disulfide.[24] As society is rapidly moving towards a more sustainable future, building blocks from more environmentally sustainable feedstocks should be considered for promoting sustainability in next-generation conjugated polymers. Furans are among the few conjugated moieties that are easily derived from bio renewable resources (**Figure S1**). Furfural, a precursor to furan, can be produced via the acid-catalyzed digestion of hemicellulose-rich agricultural wastes.[25] The C5 polysaccharides from this hemicellulose-rich agricultural waste is then hydrolyzed to monosaccharides by an acid catalyst, which are further dehydrated to afford furfural. Corncobs and bagasse from sugar cane are some of the major industrial feedstocks for furfural production.[26]

Although conjugated polymers with furan substitution typically show lower mobility compared to thiophene, it is still possible to achieve high mobilities.[27–29] In DPP-based conjugated polymers, various furan moieties have been incorporated as the flanking or non-flanking units; however, scarce examples have been used as the non-flanking units which includes furan[28–31] and (*E*)-1,2-di(furan-2-yl)ethene (**Figure S2**).[32,33] Broadly speaking, due to the lack of furan-based moieties for high-mobility conjugated polymers, different methods of furan incorporation need to be investigated to develop coherent structure–morphology–performance relationships; such knowledge will establish guidelines for the future development of sustainable, furan-based conjugated materials, in a similar fashion to what has been accomplished for the prevailing thiophene building blocks.

With the ultimate goal of developing high performance conjugated polymers having greater potential of being sourced from environmental feedstocks, we herein selected a high-mobility DPP-based conjugated polymer to construct a series of polymers that have furan moieties at different position of the repeating unit (**Figure 1**), and systematically studied the effect on the microstructure and charge transport of these structurally related conjugated polymers. Specifically, furan is incorporated at two varying positions within the polymer backbone: flanking the electron deficient DPP unit or as non-flanking units.

This article is protected by copyright. All rights reserved.

The characteristics of the four polymers are elucidated via optical/physical properties and microstructure analyses. The thiophene-based reference material, P(**T**DPP-2**T**), shows an optimized mobility of 4.02×10^{-1} $cm^2\ V^{-1}\ s^{-1}$ while the (all) furan-based material, P(**F**DPP-2**F**), shows an expected decrease in mobility to 4.03×10^{-2} $cm^2\ V^{-1}\ s^{-1}$. Interestingly, the polymers with mixed furan-thiophene units show vastly different mobilities: while P(**T**DPP-2**F**) displays an optimized mobility of 3.05×10^{-1} $cm^2\ V^{-1}\ s^{-1}$, P(**F**DPP-2**T**) shows a reduced mobility of 9.23×10^{-2} $cm^2\ V^{-1}\ s^{-1}$. The observed changes in OFET performance due to furan incorporation can be ascribed to electronic structure or film morphological differences, highlighting the importance of proper furan incorporation into the conjugated backbone.

RESULTS AND DISCUSSION

Design and Synthesis

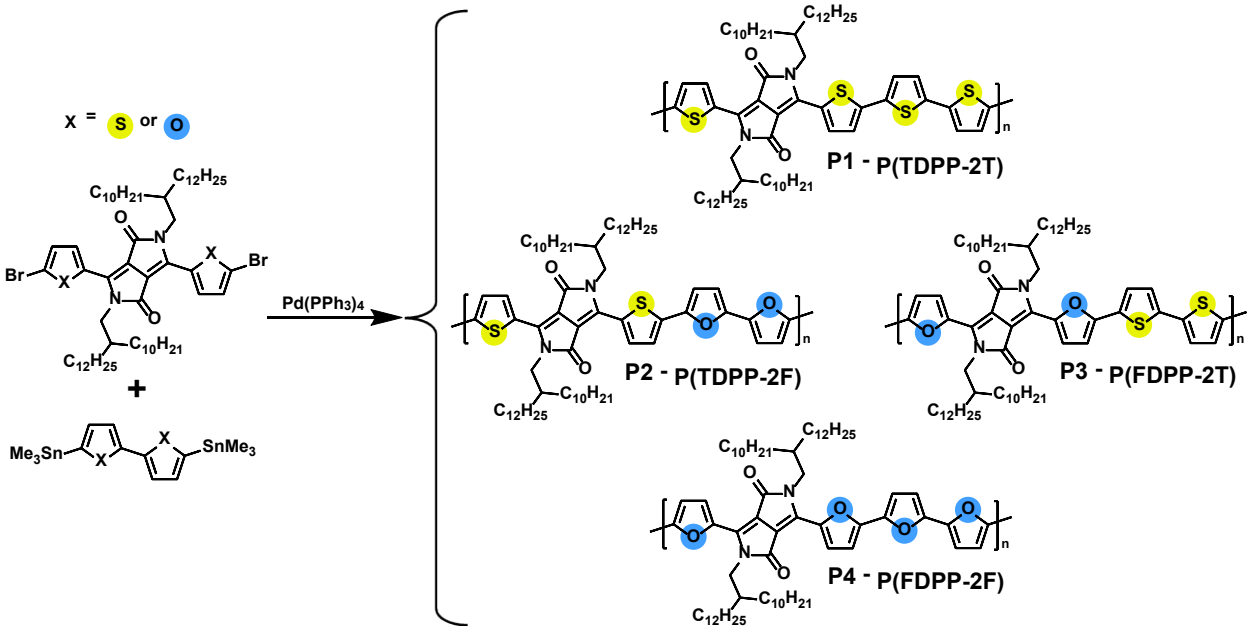

Figure 1. Design and synthesis of the four polymers in this work, with P2 and P3 being structural isomers.

This article is protected by copyright. All rights reserved.

Accepted Manuscript

1864564x, ja, Downloaded from https://chemistry-europe.onlinelibrary.wiley.com/doi/10.1002/cssc.202400171 by Argonne National Laboratory, Wiley Online Library on [25/03/2024]. See the Terms and Conditions (https://onlinelibrary.wiley.com/terms-and-conditions) on Wiley Online Library for rules of use; OA articles are governed by the applicable Creative Commons License

1864564x, ja, Downloaded from https://chemistry-europe.onlinelibrary.wiley.com/doi/10.1002/cssc.202400171 by Argonne National Laboratory, Wiley Online Library on [25/03/2024]. See the Terms and Conditions (https://onlinelibrary.wiley.com/terms-and-conditions) on Wiley Online Library for rules of use; OA articles are governed by the applicable Creative Commons License

Accepted Manuscript

Our design was focused on the DPP-quaterthiophene copolymer structure as it is a commonly used architecture for high-mobility systems.[18,34–36] In comparison to the all-thiophene reference material P(TDPP-2T), three derivatives were designed (**Figure 1**): two polymers bearing mixed thiophene and furan units that differ in their positioning, (P(TDPP-2F), P(FDPP-2T)), and one completely comprised of furan (P(FDPP-2F)). All polymers were designed to possess the same solubilizing side chain, to minimize any impact from varying the side chain and focus on the impacts induced by the different conjugated backbone. The two different DPP-based monomers with either flanking thiophenes or furans were synthesized according to previous literature.[18,37] The stannylated bifuran monomer was synthesized via oxidative homocoupling of furan, followed by subsequent stannylation. Finally, all polymers were synthesized via a microwave-assisted Stille polymerization.[38,39] The number-average molar mass (M_n) and dispersity ($Đ$) of the four polymers were measured by high-temperature gel permeation chromatography (GPC). The M_n of all four polymers were relatively similar; ranging from 40k to 59k. Synthetic details and corresponding characterizations are included in the Supporting Information, where a hypothetical synthetic scheme of the furan-based materials from bio-sourced feedstocks is shown in **Figure S1**.

To investigate the impact of furan incorporation on the structural conformations of the polymers, geometry-optimized structures were simulated using density functional theory (DFT) with the B3LYP/6-31G* basis set. The respective repeating units were used as model molecules in a sequential manner with the alkyl side chain being removed for simplicity. Replacing thiophene with furan in a conjugated molecule is expected to result in more planar structure as compared to the S atom, since O has a smaller radius and a shorter C-O bond length.[40] Also, furan has reduced aromaticity compared to thiophene, which impacts how furan moieties behave within larger conjugated systems.[41,42] Our calculations disclose different torsional angles between neighboring aromatic units in the repeat unit for each polymer (**Figure S4**); interestingly, the TDPP-2F (calculated torsional angles of 0.0 °, 0.0 ° and 0.0 °) repeat unit is more planar compared to FDPP-2T (calculated torsional angles of 0.0 °, 1.3 ° and 18.6 °), which is in agreement with previous studies.[43] It is expected that changes in the dihedral angles of the polymer backbone will result in differences in the optoelectronic, morphological and transport properties.

This article is protected by copyright. All rights reserved.

1864564x, ja, Downloaded from https://chemistry-europe.onlinelibrary.wiley.com/doi/10.1002/cssc.202400171 by Argonne National Laboratory, Wiley Online Library on [25/03/2024]. See the Terms and Conditions (https://onlinelibrary.wiley.com/terms-and-conditions) on Wiley Online Library for rules of use; OA articles are governed by the applicable Creative Commons License

Accepted Manuscript

Optical and Electrochemical Properties

Morphological optimization of the semiconductor layer in the thin film-based OFETs require a comprehensive understanding of the aggregation of conjugated polymers in solution and solid states; optical spectroscopy is a common method used to investigate polymer aggregation in solution or film state.[44] The absorption of the four different polymers in their chloroform (CF) solution are shown in **Figure 2a** and summarized in **Table 1**. In the absorption profiles, the four polymers exhibited broad absorption features with two distinct peaks in the region of 300 nm to 950 nm. The shorter wavelength peaks at around 300-450 nm are ascribed to the π-π* transition bands, while those between 500-950 nm correspond to the intramolecular charge transfer (ICT) bands. Focusing on the ICT band, the all thiophene-based polymer P(TDPP-2T) possesses a λ_{max} at 775 nm, with an absorbance onset at 910 nm; by contrast, the mixed thiophene-furan polymers P(TDPP-2F) and P(FDPP-2T) show an absorbance profile with more distinct 0-0 and 0-1 vibronic transitions in solution compared to the all thiophene polymer, P(TDPP-2T). Interestingly, the furan unit positioning does not significantly impact the optical properties in solution as P(TDPP-2F) and P(FDPP-2T) – two structural isomers – had similar absorption profiles. However, the mixed thiophene-furan polymers, P(TDPP-2F) and P(FDPP-2T), show a blue-shifted absorption onset of 810 nm and 805 nm respectively, representing a shift of around 100 nm compared to P(TDPP-2T), the all thiophene-based polymer. Thus, the optical band gap (E_g^{opt}) as estimated from the absorption onset increased with the incorporation of furan into the polymer backbone. This is further demonstrated as the all furan-based polymer P(FDPP-2F) shows a further, blue-shifted absorption profile with a λ_{max} at 670 nm and 737 nm, and an absorption onset at 790 nm.

This article is protected by copyright. All rights reserved.

10.1002/cssc.202400171

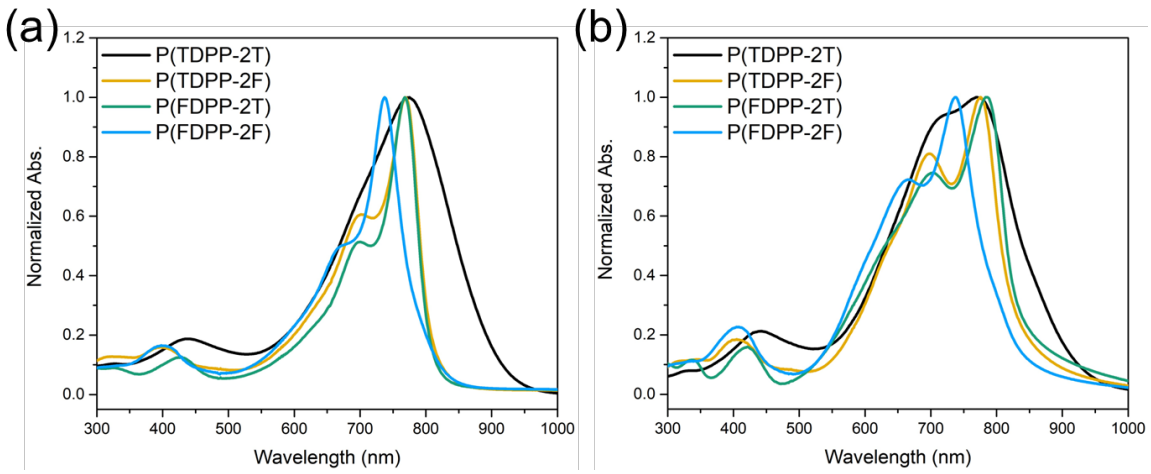

Figure 2. Normalized UV-Vis absorption spectra in (a) CF solution; (b) films.

Table 1. Summary of the optical and electrochemical properties of the polymers determined in CF solution and film states cast from CF.

Polymer	Solution		Film				
	λ_{max}^{Sol} (nm)	λ_{onset}^{Sol} (nm)	λ_{max} (nm)	λ_{onset} (nm)	E_g^{opt} (eV)	[a]HOMO^{CV} (eV)	[b]LUMO (eV)
P(TDPP-2T)	775	910	718, 769	925	1.34	-5.23	-3.89
P(TDPP-2F)	702, 769	810	768, 775	830	1.50	-5.27	-3.77
P(FDPP-2T)	700, 768	805	703, 784	835	1.49	-5.37	-3.88
P(FDPP-2F)	670, 737	790	667, 738	825	1.51	-5.34	-3.83

[a]Calculated from the E_{OX}. [b]Calculated from the HOMO + E_g^{opt}. The E_{OX} was determined from the CV measurement where a 0.1 M tetrabutylammonium hexafluorophosphate in acetonitrile solution was used as supporting electrolyte.

The absorption properties of all four polymers as thin films were further measured, which represent the aggregated polymers in the solid state. Differences in the absorption profiles remain present and consistent with the results obtained in solution. However, when transitioning from solution to film states, the absorption spectra of all the polymers in the film states are slightly broader with small chromatic shifts compared to solution, implying that there are fewer changes in the backbone conformations of the polymers in solution compared to thin films.[30] All four polymers exhibit a minor red shift (15 nm – 35 nm) in the

This article is protected by copyright. All rights reserved.

Accepted Manuscript

1864564x, ja, Downloaded from https://chemistry-europe.onlinelibrary.wiley.com/doi/10.1002/cssc.202400171 by Argonne National Laboratory, Wiley Online Library on [25/03/2024]. See the Terms and Conditions (https://onlinelibrary.wiley.com/terms-and-conditions) on Wiley Online Library for rules of use; OA articles are governed by the applicable Creative Commons License

absorption onset (λ_{onset}) when transitioning from solution to film. From the absorption onset, the optical band gap can be estimated by $E_g^{opt} = 1240/ \lambda_{onset}$. Unsurprisingly, P(TDPP-2T) possessed the smallest E_g^{opt} of 1.34 eV. Interestingly, all three other polymers containing furan showed increased band gaps of around 1.50 eV. All optical properties are summarized in **Table 1**.

To further evaluate the incorporation of furan on the energy levels of this polymer series, we applied cyclic voltammetry (CV) to estimate the highest occupied molecular orbital (HOMO) energy levels (**Figure S5**). The HOMO energy levels can be calculated from the conversion of the oxidation onset (E_{OX}) through the ferrocene standard (E_{FC}) using the equation HOMO = – (4.8+(E_{OX}-E_{FC})). As the reduction onsets (E_{RED}) were difficult to identify (commonly observed for p-type conjugated polymers), the LUMO levels were estimated using the equation LUMO = $HOMO^{CV}$ + E_g^{opt}. The HOMO and LUMO levels of P(TDPP-2T) were estimated to be – 5.23 eV and – 3.89 eV, respectively, and the energy levels of other three polymers were determined similarly. It was found that the HOMO levels were deepened for all three polymers incorporating furan. Interestingly, the HOMO level of P(TDPP-2F) is more similar to that of P(TDPP-2T), while the HOMO levels of P(FDPP-2T) and P(FDPP-2F) are further deepened. This indicates that the donor-acceptor effect between the DPP and flanking aromatic unit has a stronger impact on the HOMO energy level compared to the non-flanking units.

This article is protected by copyright. All rights reserved.

Accepted Manuscript

1864564x, ja, Downloaded from https://chemistry-europe.onlinelibrary.wiley.com/doi/10.1002/cssc.202400171 by Argonne National Laboratory, Wiley Online Library on [25/03/2024]. See the Terms and Conditions (https://onlinelibrary.wiley.com/terms-and-conditions) on Wiley Online Library for rules of use; OA articles are governed by the applicable Creative Commons License

1864564x, ja, Downloaded from https://chemistry-europe.onlinelibrary.wiley.com/doi/10.1002/cssc.202400171 by Argonne National Laboratory, Wiley Online Library on [25/03/2024]. See the Terms and Conditions (https://onlinelibrary.wiley.com/terms-and-conditions) on Wiley Online Library for rules of use; OA articles are governed by the applicable Creative Commons License

Accepted Manuscript

Thermal and Morphological Characteristics

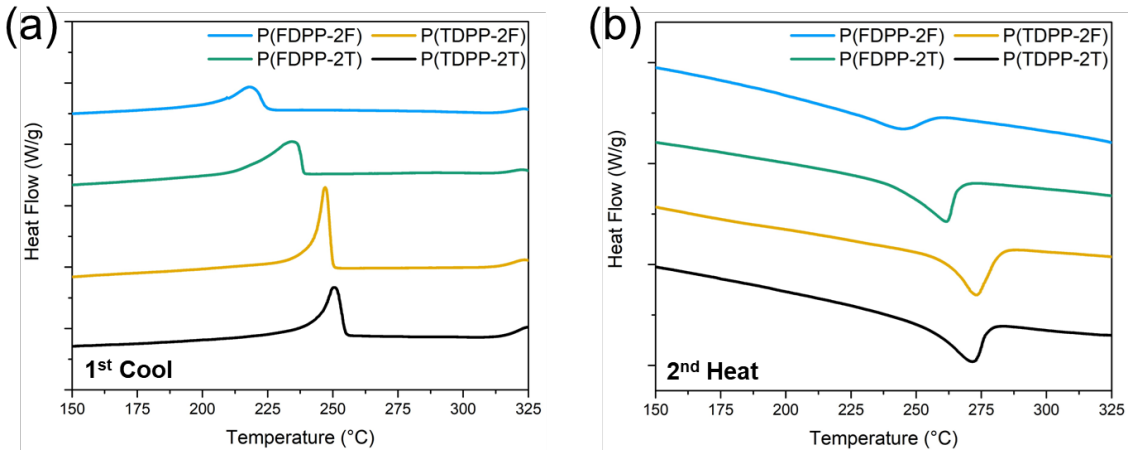

Figure 3. DSC heating and cooling traces of the DPP polymers at a scan rate of 10 °C/min under N_2 (exo up). (a) first cooling; (b) second heating cycles.

Differential scanning calorimetry (DSC) and thermogravimetric analysis (TGA) were used to assess the thermal properties of the four polymers. DSC was used to study the thermal transition behavior of the DPP polymers at high temperatures while TGA was used to assess the stability of the polymers. TGA showed that all four polymers have good thermal stability with a 5% weight loss temperature around 400 °C (**Figure S7**). All four polymers show melt and crystalline peaks above 200 °C during the heating and cooling process, respectively. The heats of crystallization (ΔH_c) and melting (ΔH_m) calculated from the DSC thermograms are shown in **Figure 3** and summarized in **Table 2**. Full DSC scans are shown in **Figure S6**. The reference polymer P(TDPP-2T) showed a T_c and T_m of 250.5 °C and 271.5 °C, respectively.[14] From these transitions, we calculated that P(TDPP-2T) produced a ΔH_c and ΔH_m of 8.88 J/g and 5.45 J/g, respectively. By contrast, the all-furan polymer, P(FDPP-2F) exhibited peaks with lower intensity, as evidenced from the reduced T_c, T_m, ΔH_c and ΔH_m. This reduction is likely attributed to weaker crystallites and lower crystallinity within P(FDPP-2F) as compared to P(TDPP-2T).[45] Interestingly, P(TDPP-2F) showed a larger ΔH_c and ΔH_m of 11.49 J/g and 7.78 J/g, respectively, compared to P(TDPP-2T). On the other hand, P(FDPP-2T) (the structural isomer to P(TDDP-2F)) showed reduced transition temperatures

This article is protected by copyright. All rights reserved.

followed by reduced ΔH_c and ΔH_m values compared to P(TDPP-2F), owing to the reduced crystallinity. This difference may be attributed to the increased in planarity of the polymer backbone of P(TDPP-2F) compared to P(FDPP-2T) (**Figure S4**).

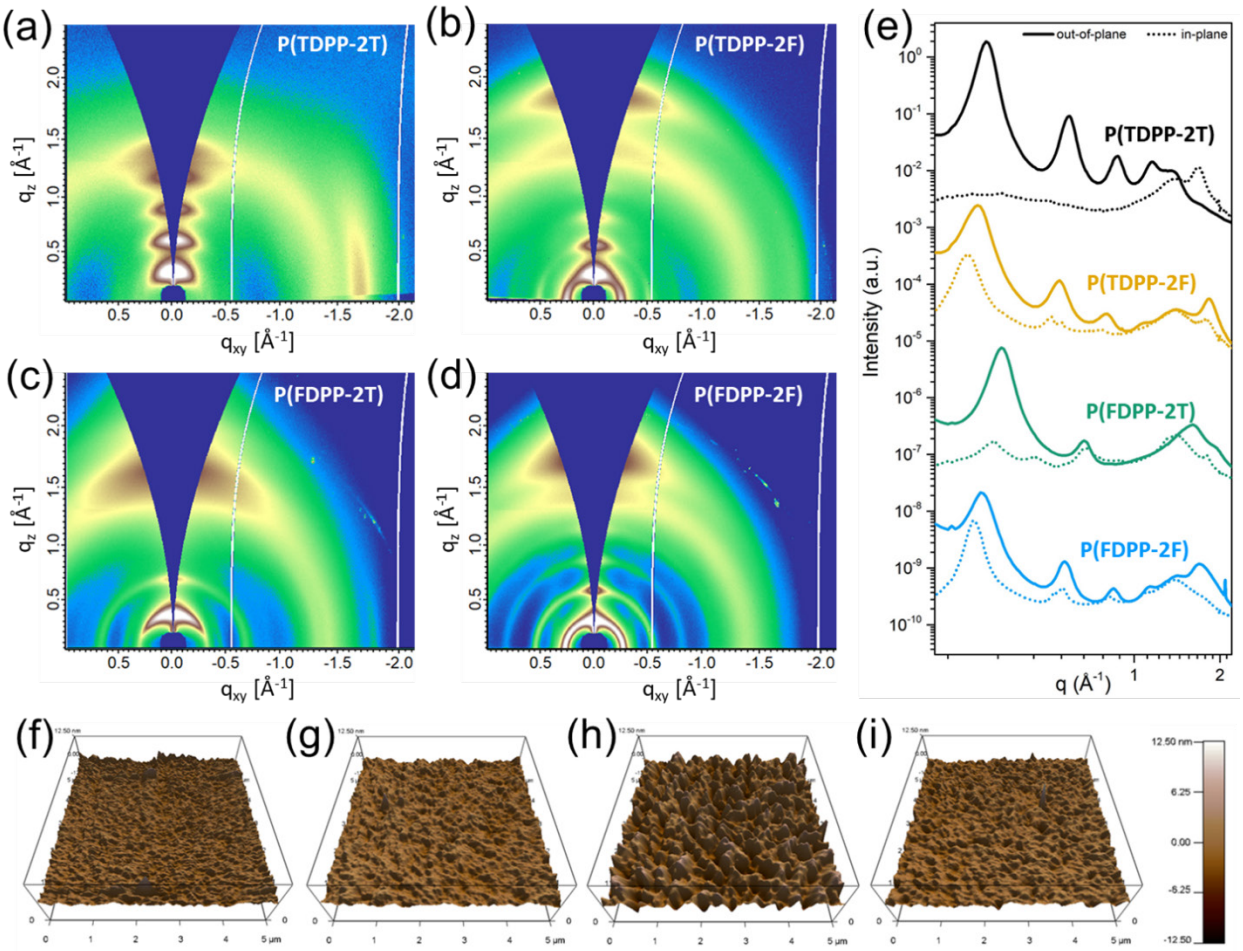

Figure 4. 2D-GIWAXS and 3D-AFM (5 μm × 5 μm) images of the DPP polymer thin films fabricated from a $CHCl_3$:*o*-DCB (9/1, v/v) mix solution. (a,f) P(TDPP-2T); (b,g) P(TDPP-2F); (c,h) P(FDPP-2T); (d,i) P(FDPP-2F); (e) OOP and IP line cut profiles of the corresponding 2D-GIWAXS patterns.

This article is protected by copyright. All rights reserved.

1864564x, ja, Downloaded from https://chemistry-europe.onlinelibrary.wiley.com/doi/10.1002/cssc.202400171 by Argonne National Laboratory, Wiley Online Library on [25/03/2024]. See the Terms and Conditions (https://onlinelibrary.wiley.com/terms-and-conditions) on Wiley Online Library for rules of use; OA articles are governed by the applicable Creative Commons License

Accepted Manuscript

1864564x, ja, Downloaded from https://chemistry-europe.onlinelibrary.wiley.com/doi/10.1002/cssc.202400171 by Argonne National Laboratory, Wiley Online Library on [25/03/2024]. See the Terms and Conditions (https://onlinelibrary.wiley.com/terms-and-conditions) on Wiley Online Library for rules of use; OA articles are governed by the applicable Creative Commons License

Table 2. Summarized thermal properties of the four polymers and GIWAXS summary of neat polymer films.

Polymer	T_c (°C)	ΔH_c (J/g)	T_m (°C)	ΔH_m (J/g)	[a]Out-of-plane (100)		[a]In-plane (010)	
					q_z ($Å^{-1}$)	d-spacing (Å)	q_{xy} ($Å^{-1}$)	π-π distance (Å)
P(TDPP-2T)	250.5	8.88	271.5	5.45	0.304	20.7	1.67	3.76
P(TDPP-2F)	247.0	11.49	273.1	7.78	0.281	22.4	1.77	3.55
P(FDPP-2T)	234.2	9.36	261.5	5.72	0.343	18.3	- -	- -
P(FDPP-2F)	218.0	6.63	245.6	2.04	0.291	21.6	- -	- -

[a]Thin films fabricated from a $CHCl_3$:*o*-DCB (9/1, v/v) mix solution annealed at 150 °C for 10 min for GIWAXS analysis.

To evaluate the incorporation of furan into the polymer backbone on the molecular self-assembly and orientational features of the films, atomic force microscopy (AFM) and grazing incidence wide-angle X-ray scattering (GIWAXS) was conducted for thin films of pure polymers (**Figure 4**). The AFM height images are shown in **Figure 4f-i** and **Figure S8**, respectively. All polymers show a relatively similar surface roughness (~ 1 nm) except that P(FDPP-2T) is slightly rougher (~ 2 nm). On the other hand, the crystallographic parameters obtained from GIWAXS are shown in **Table 2** and **Table S3-S4**. All annealed films show some degree of ordered lamellar (h00) Bragg peaks along the q_z axes. For the all-thiophene reference polymer P(TDPP-2T), a d-spacing of 20.7 Å is observed with distinct (h00) diffraction peaks up to the fourth order in the out-of-plane (OOP) direction. A π–π stacking distance of 3.76 Å is observed from the 010 peak in the in-plane (IP) direction. Thus, this all thiophene polymer shows a highly ordered and edge-on preference with respect to the substrate, resulting in a favorable morphology for horizontal transport (i.e., preferred orientation for OFETs). On the other hand, it is observed that addition of furan into the conjugated backbone leads to a more bimodal packing, with mixed edge-on and face-on orientations of the polymeric chains relative to the substrate. This can be seen by the (010) peak in the OOP direction for P(TDPP-2F) while there is still some amount of π–π stacking in the IP direction. A close π–π stacking

This article is protected by copyright. All rights reserved.

Accepted Manuscript

1864564x, ja, Downloaded from https://chemistry-europe.onlinelibrary.wiley.com/doi/10.1002/cssc.202400171 by Argonne National Laboratory, Wiley Online Library on [25/03/2024]. See the Terms and Conditions (https://onlinelibrary.wiley.com/terms-and-conditions) on Wiley Online Library for rules of use; OA articles are governed by the applicable Creative Commons License

Accepted Manuscript

distance of 3.55 Å is observed in the IP direction, while an increased d-spacing of 22.4 Å is observed in the OOP direction with diffraction peaks to the third order for P(TDPP-2F). Although this polymer P(TDPP-2F) shows less consistent order compared to P(TDPP-2T), the reduction in the π–π stacking distance would be favorable to facilitate charge transport.

In a similar vein, polymers P(FDPP-2T) and P(FDPP-2F) once again show unfavorable bimodal distributions as they possessed OOP d-spacings of 18.3 Å and 21.6 Å, respectively, with no obvious IP π–π stacking peaks. It is interesting to note that the two polymers with bifuran units (2F) (i.e., P(TDPP-2F) and P(FDPP-2F)) show increased d-spacing distances, indicating less side chain interdigitation and bimodal d-spacings in both IP and OOP as seen by the line-cut profiles in **Figure 4e**. Since these two structural isomers, P(TDPP-2F) and P(FDPP-2T), are comprised of both thiophene and furan units, it is observed that replacing the flanking thiophene units with furan (i.e., P(FDPP-2T) vs. P(TDPP-2T)), as opposed to the non-flanking units (i.e., P(TDPP-2F) vs P(TDPP-2T)), has a more detrimental impact on the polymer morphology. Since an edge-on preference is favorable for horizontal charge transfer in OFETs,[46–48] it can be inferred that P(TDPP-2T) and P(TDPP-2F) would show improved transport characteristics.

This article is protected by copyright. All rights reserved.

10.1002/cssc.202400171

Field-Effect Transistor (FET) Characteristics

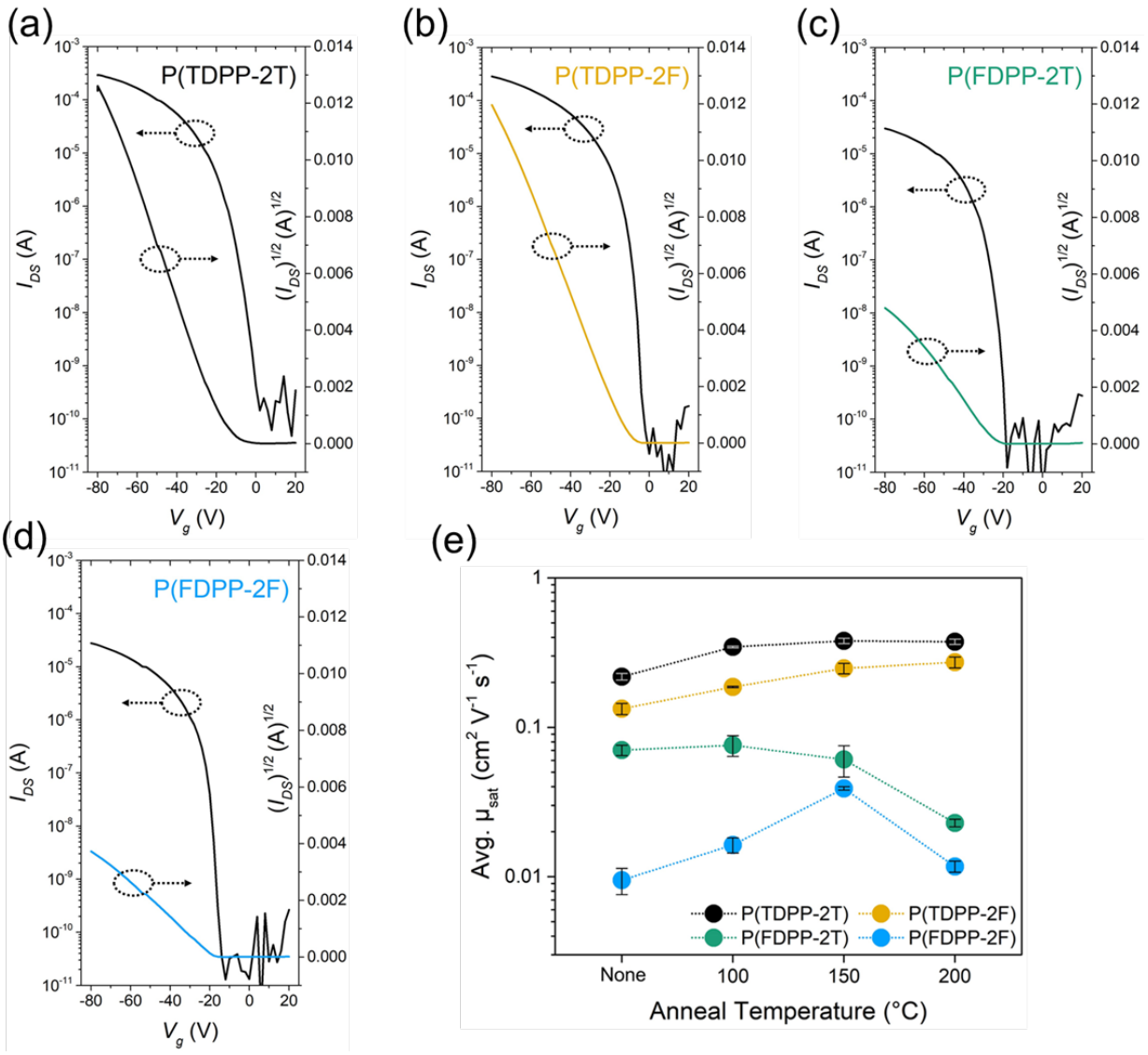

Figure 5. Transfer characteristics of optimized BGTC transistors. (a) P(TDPP-2T); (b) P(TDPP-2F); (c) P(FDPP-2T); (d) P(FDPP-2F); The average hole mobilities of studied polymers from at least three devices at various annealing conditions. Error bars denote standard deviations. Dashed lines serve as a guide to the eye.

To investigate the relationship between the incorporation of furan into the conjugated polymer backbone and charge transport characteristics, bottom-gate/top-contact FET devices were fabricated. 300 nm thick SiO_2 dielectric layer of highly p-doped silicon substrate was modified with octadecyltrimethoxysilane (OTS) to enhance the electrical performance. The polymer films were prepared by spin coating the polymer solution from a $CHCl_3$:*o*-DCB (9/1, v/v) mix solution followed by annealing

This article is protected by copyright. All rights reserved.

Accepted Manuscript

1864564x, ja, Downloaded from https://chemistry-europe.onlinelibrary.wiley.com/doi/10.1002/cssc.202400171 by Argonne National Laboratory, Wiley Online Library on [25/03/2024]. See the Terms and Conditions (https://onlinelibrary.wiley.com/terms-and-conditions) on Wiley Online Library for rules of use; OA articles are governed by the applicable Creative Commons License

1864564x, ja, Downloaded from https://chemistry-europe.onlinelibrary.wiley.com/doi/10.1002/cssc.202400171 by Argonne National Laboratory, Wiley Online Library on [25/03/2024]. See the Terms and Conditions (https://onlinelibrary.wiley.com/terms-and-conditions) on Wiley Online Library for rules of use; OA articles are governed by the applicable Creative Commons License

Accepted Manuscript

at a respective temperature. The optimized *p*-channel transfer characteristics are depicted in **Figure 5a-e**, and the device performance parameters are summarized in **Table 3**. The full summary of FET characteristics is given in the supplemental **Figures S9-S12** and **Table S5**. All devices show relatively linear FET transfer characteristic (I_{SD} (VG) and $|I_{SD}|^{1/2}$ (VG)) dependencies in saturation regimes.[49] It is observed that P(TDPP-2T) and P(FDPP-2F) exhibit the optimized mobility with the thin films annealed at 150 °C, while P(TDPP-2F) and P(FDPP-2T) required annealing their thin films at 200 °C and 100 °C, respectively, to obtain the optimized mobilities (**Table S5**, Supporting Information).

As expected, the all-thiophene reference polymer P(TDPP-2T), due to its favorable edge-on morphology, showed the highest hole mobility of 3.79×10^{-1} cm^2 V^{-1} s^{-1} with an I_{on}/I_{off} ratio of $>10^6$ at the optimized condition. On the other hand, the all-furan polymer, P(FDPP-2F) would yield decreased transport characteristics due to its less favorable electronic structure and morphological properties. Indeed, a lower average mobility of 3.81×10^{-2} cm^2 V^{-1} s^{-1} with an I_{on}/I_{off} ratio of $>10^5$ was obtained for P(FDPP-2F) at the optimized condition. It should be noted that the transport characteristics of P(FDPP-2F) were more sensitive to the various annealing conditions compared to P(TDPP-2T), which is likely attributed to changes in the morphology upon the different annealing temperatures. As for the mixed thiophene-furan polymers, P(TDPP-2F) showed a high average mobility of 2.73×10^{-1} cm^2 V^{-1} s^{-1} with an I_{on}/I_{off} ratio of $>10^6$, while P(FDPP-2T) showed an average mobility of 7.58×10^{-2} cm^2 V^{-1} s^{-1} with an I_{on}/I_{off} ratio of $>10^5$ at their optimized conditions. These results are expected as P(TDPP-2F) shows increased planarity, improved thermal and morphological characteristics, leading to improved charge transport compared to P(FDPP-2T). It is interesting to note that all-furan-based DPP polymers typically outperform the mixed thiophene-furan variants in literature reports (**Figure S2**);[27,29,30,32] however, the all-furan-based DPP polymer in our study exhibited the lower mobility. Nevertheless, the observed differences in mobilities of these four polymers in our study indicate the importance of having thiophene units flank the DPP core as the two TDPP-based polymers consistently showed higher mobility than the FDPP-based ones (**Figure 5e**). Furthermore, our results indicate the importance of the optimized incorporation and placement of furan as P(TDPP-2F) shows nearly comparable performance to the reference polymer, P(TDPP-2T).

This article is protected by copyright. All rights reserved.

1864564x, ja, Downloaded from https://chemistry-europe.onlinelibrary.wiley.com/doi/10.1002/cssc.202400171 by Argonne National Laboratory, Wiley Online Library on [25/03/2024]. See the Terms and Conditions (https://onlinelibrary.wiley.com/terms-and-conditions) on Wiley Online Library for rules of use; OA articles are governed by the applicable Creative Commons License

Table 3. Summary of optimized field-effect transistor (FET) characteristics of the DPP polymers.

Polymer	Max μ_{sat} ($cm^2 V^{-1} s^{-1}$)	[d]Avg. μ_{sat} ($cm^2 V^{-1} s^{-1}$)	[e]I_{on}/I_{off}	[f]V_{th} (V)
[a]P(TDPP-2T)	4.02×10^{-1}	3.79×10^{-1}	$>10^6$	-12
[b]P(TDPP-2F)	3.05×10^{-1}	2.73×10^{-1}	$>10^6$	-11
[c]P(FDPP-2T)	9.23×10^{-2}	7.58×10^{-2}	$>10^5$	-26
[a]P(FDPP-2F)	4.03×10^{-2}	3.81×10^{-2}	$>10^5$	-21

[a]Annealed at 150 °C for 10 min. [b]Annealed at 200 °C for 10 min. [c]Annealed at 100 °C for 10 min. [d]Average mobilities of studied polymers from at least three devices. [e]Current on/off ratio. [f]Threshold voltage.

CONCLUSIONS

With the goal of developing derivates having greater potential of being sourced from environmental feedstocks, we selectively introduce furan into a DPP-based reference conjugated polymer to systematically study the effect on the chain conformation, electronic structure, microstructure and charge transport of conjugated polymers. Specifically, furan is incorporated at two varying positions within the polymer backbone; flanking the electron deficient DPP unit or non-flanking units. The characteristics of the four polymers are elucidated via optical/physical properties and microstructure analyses. DFT calculations revealed a more planar backbone for polymers with bifuran units. GIWAXS and thermal analysis revealed a more preferential morphology for P(TDPP-2T) and P(TDPP-2F), while P(FDPP-2T) and P(FDPP-2F) show less favorable morphologies with reduced order. As expected, the all furan-based material P(FDPP-2F), shows a decreased maximum mobility of 4.03×10^{-2} cm^2 V^{-1} s^{-1}. Contrary to previous examples, the polymers with mixed furan-thiophene units show improved mobilities over the all-furan polymer, as P(TDPP-2F) exhibits an optimized maximum mobility of 3.05×10^{-1} cm^2 V^{-1} s^{-1} and P(FDPP-2T), shows a reduced maximum mobility of 9.23×10^{-2} cm^2 V^{-1} s^{-1}, highlighting the importance of optimized furan incorporation.

This article is protected by copyright. All rights reserved.

Accepted Manuscript

1864564x, ja, Downloaded from https://chemistry-europe.onlinelibrary.wiley.com/doi/10.1002/cssc.202400171 by Argonne National Laboratory, Wiley Online Library on [25/03/2024]. See the Terms and Conditions (https://onlinelibrary.wiley.com/terms-and-conditions) on Wiley Online Library for rules of use; OA articles are governed by the applicable Creative Commons License

Accepted Manuscript

In conclusion, we show that partially and selectively replacing thiophene units with furan can yield nearly comparable performance compared to the all-thiophene polymer. This strategy offers an improvement in the sustainability of the polymer by using bio-sourced furan without sacrificing the high-performance characteristics. The changes in OEFT performance due to furan incorporation can be ascribed to a combination of electronic and morphological differences, highlighting the importance of proper furan incorporation into the conjugated backbone.

ASSOCIATED CONTENT

Supporting Information

The Supporting Information is available and includes methods, detailed synthetic procedures, detailed device fabrication and additional CV, DSC, TGA, AFM, and GIWAXS data.

ACKNOWLEDGMENTS

This work was financially supported by the National Science Foundation (NSF) under Award CMMI-2134664. Work performed at the Center for Nanoscale Materials, a U.S. Department of Energy Office of Science User Facility, was supported by the U.S. DOE, Office of Basic Energy Sciences, under Contract No. DE-AC02-06CH11357. Work at the Center for Nanoscale Materials was completed under proposal CNM 81596. NMR Spectrometers were supported by the National Science Foundation under Grant No. CHE-0922858 and CHE-1828183. The authors thank Amar S. Kumbhar for conducting AFM measurements.

This article is protected by copyright. All rights reserved.

1864564x, ja, Downloaded from https://chemistry-europe.onlinelibrary.wiley.com/doi/10.1002/cssc.202400171 by Argonne National Laboratory, Wiley Online Library on [25/03/2024]. See the Terms and Conditions (https://onlinelibrary.wiley.com/terms-and-conditions) on Wiley Online Library for rules of use; OA articles are governed by the applicable Creative Commons License

Accepted Manuscript

REFERENCES

(1) Someya, T.; Bao, Z.; Malliaras, G. G. The Rise of Plastic Bioelectronics. *Nature* **2016**, *540* (7633), 379–385. https://doi.org/10.1038/nature21004.

(2) Bao, Z.; Chen, X. Flexible and Stretchable Devices. *Adv. Mater.* **2016**, *28* (22), 4177–4179. https://doi.org/10.1002/adma.201601422.

(3) Li, J.; Zhao, Y.; Tan, H. S.; Guo, Y.; Di, C. A.; Yu, G.; Liu, Y.; Lin, M.; Lim, S. H.; Zhou, Y.; Su, H.; Ong, B. S. A Stable Solution-Processed Polymer Semiconductor with Record High-Mobility for Printed Transistors. *Sci. Rep.* **2012**, *2*, 1–9. https://doi.org/10.1038/srep00754.

(4) Lu, L.; Wang, D.; Pu, C.; Cao, Y.; Li, Y.; Xu, P.; Chen, X.; Liu, C.; Liang, S.; Suo, L.; Cui, Y.; Zhao, Z.; Guo, Y.; Liang, J.; Liu, Y. High-Performance Flexible Organic Field Effect Transistors with Print-Based Nanowires. *Microsystems Nanoeng.* **2023**, *9* (1). https://doi.org/10.1038/s41378-023-00551-x.

(5) Bucella, S. G.; Luzio, A.; Gann, E.; Thomsen, L.; McNeill, C. R.; Pace, G.; Perinot, A.; Chen, Z.; Facchetti, A.; Caironi, M. Macroscopic and High-Throughput Printing of Aligned Nanostructured Polymer Semiconductors for MHz Large-Area Electronics. *Nat. Commun.* **2015**, *6* (8394). https://doi.org/10.1038/ncomms9394.

(6) Tsumura, A.; Koezuka, H.; Ando, T. Macromolecular Electronic Device: Field-Effect Transistor with a Polythiophene Thin Film. *Appl. Phys. Lett.* **1986**, *49* (18), 1210–1212. https://doi.org/10.1063/1.97417.

(7) Dong, H.; Fu, X.; Liu, J.; Wang, Z.; Hu, W. 25th Anniversary Article: Key Points for High-Mobility Organic Field-Effect Transistors. *Adv. Mater.* **2013**, *25* (43), 6158–6183. https://doi.org/10.1002/adma.201302514.

(8) Sirringhaus, H. 25th Anniversary Article: Organic Field-Effect Transistors: The Path beyond Amorphous Silicon. *Adv. Mater.* **2014**, *26* (9), 1319–1335. https://doi.org/10.1002/adma.201304346.

(9) Yang, Y.; Liu, Z.; Chen, J.; Cai, Z.; Wang, Z.; Chen, W.; Zhang, G.; Zhang, X.; Chi, L.; Zhang, D. A Facile Approach to Improve Interchain Packing Order and Charge Mobilities by Self-Assembly of Conjugated Polymers on Water. *Adv. Sci.* **2018**, *5* (11), 1–8. https://doi.org/10.1002/advs.201801497.

(10) Lee, J.; Kang, S. H.; Lee, S. M.; Lee, K. C.; Yang, H.; Cho, Y.; Han, D.; Li, Y.; Lee, B. H.; Yang, C. An Ultrahigh Mobility in Isomorphic Fluorobenzo[c][1,2,5]Thiadiazole-Based Polymers. *Angew. Chemie - Int. Ed.* **2018**, *57* (41), 13629–13634. https://doi.org/10.1002/anie.201808098.

(11) Kim, G.; Kang, S. J.; Dutta, G. K.; Han, Y. K.; Shin, T. J.; Noh, Y. Y.; Yang, C. A Thienoisoindigo-Naphthalene Polymer with Ultrahigh Mobility of 14.4 Cm2/V·s That Substantially Exceeds Benchmark Values for Amorphous Silicon Semiconductors. *J. Am. Chem. Soc.* **2014**, *136* (26), 9477–9483. https://doi.org/10.1021/ja504537v.

(12) Back, J. Y.; Yu, H.; Song, I.; Kang, I.; Ahn, H.; Shin, T. J.; Kwon, S. K.; Oh, J. H.; Kim, Y. H. Investigation of Structure-Property Relationships in Diketopyrrolopyrrole-Based Polymer Semiconductors via Side-Chain Engineering. *Chem. Mater.* **2015**, *27* (5), 1732–1739. https://doi.org/10.1021/cm504545e.

(13) Neu, J.; Samson, S.; Ding, K.; Rech, J. J.; Ade, H.; You, W. Oligo(Ethylene Glycol) Side Chain Architecture Enables Alcohol-Processable Conjugated Polymers for Organic Solar Cells.

This article is protected by copyright. All rights reserved.

Macromolecules **2023**, No. 56, 2092–2103. https://doi.org/10.1021/acs.macromol.2c02259.

(14) Zhang, A.; Xiao, C.; Wu, Y.; Li, C.; Ji, Y.; Li, L.; Hu, W.; Wang, Z.; Ma, W.; Li, W. Effect of Fluorination on Molecular Orientation of Conjugated Polymers in High Performance Field-Effect Transistors. *Macromolecules* **2016**, *49* (17), 6431–6438. https://doi.org/10.1021/acs.macromol.6b01446.

(15) Kim, M.; Ryu, S. U.; Park, S. A.; Choi, K.; Kim, T.; Chung, D.; Park, T. Donor–Acceptor-Conjugated Polymer for High-Performance Organic Field-Effect Transistors: A Progress Report. *Adv. Funct. Mater.* **2020**, *30* (20). https://doi.org/10.1002/adfm.201904545.

(16) Nielsen, C. B.; Turbiez, M.; McCulloch, I. Recent Advances in the Development of Semiconducting DPP-Containing Polymers for Transistor Applications. *Adv. Mater.* **2013**, *25* (13), 1859–1880. https://doi.org/10.1002/adma.201201795.

(17) Bürgi, L.; Turbiez, M.; Pfeiffer, R.; Bienewald, F.; Kirner, H. J.; Winnewisser, C. High-Mobility Ambipolar near-Infrared Light-Emitting Polymer Field-Effect Transistors. *Adv. Mater.* **2008**, *20* (11), 2217–2224. https://doi.org/10.1002/adma.200702775.

(18) Li, Y.; Sonar, P.; Singh, S. P.; Soh, M. S.; Van Meurs, M.; Tan, J. Annealing-Free High-Mobility Diketopyrrolopyrrole-Quaterthiophene Copolymer for Solution-Processed Organic Thin Film Transistors. *J. Am. Chem. Soc.* **2011**, *133* (7), 2198–2204. https://doi.org/10.1021/ja1085996.

(19) Yi, Z.; Wang, S.; Liu, Y. Design of High-Mobility Diketopyrrolopyrrole-Based π-Conjugated Copolymers for Organic Thin-Film Transistors. *Adv. Mater.* **2015**, *27* (24), 3589–3606. https://doi.org/10.1002/adma.201500401.

(20) Zhou, H.; Yang, L.; You, W. Rational Design of High Performance Conjugated Polymers for Organic Solar Cells. *Macromolecules* **2012**, *45* (2), 607–632. https://doi.org/10.1021/ma201648t.

(21) Pankow, R. M.; Thompson, B. C. The Development of Conjugated Polymers as the Cornerstone of Organic Electronics. *Polymer (Guildf).* **2020**, *207* (July), 122874. https://doi.org/10.1016/j.polymer.2020.122874.

(22) Yang, J.; Zhao, Z.; Wang, S.; Guo, Y.; Liu, Y. Insight into High-Performance Conjugated Polymers for Organic Field-Effect Transistors. *Chem* **2018**, *4* (12), 2748–2785. https://doi.org/10.1016/j.chempr.2018.08.005.

(23) Cinar, M. E.; Ozturk, T. Thienothiophenes, Dithienothiophenes, and Thienoacenes: Syntheses, Oligomers, Polymers, and Properties. *Chem. Rev.* **2015**, *115* (9), 3036–3140. https://doi.org/10.1021/cr500271a.

(24) Thiophene and Thiophene Derivatives. *Van Nostrand's Sci. Encycl.* **2006**, No. 1. https://doi.org/10.1002/0471743984.vse7023.

(25) Kim, H.; Kim, J.; Won, W. Toward Economical and Sustainable Production of Renewable Plastic: Integrative System-Level Analyses. *ChemSusChem* **2022**, *15* (13). https://doi.org/10.1002/cssc.202200240.

(26) Hoydonckx, H. E.; Van Rhijn, W. M.; Van Rhijn, W.; De Vos, D. E.; Jacobs, P. A. Furfural and Derivatives. *Ullmann's Encycl. Ind. Chem.* **2007**, *d*. https://doi.org/10.1002/14356007.a12_119.pub2.

(27) Chen, M. S.; Lee, O. P.; Niskala, J. R.; Yiu, A. T.; Tassone, C. J.; Schmidt, K.; Beaujuge, P. M.; Onishi, S. S.; Toney, M. F.; Zettl, A.; Fréchet, J. M. J. Enhanced Solid-State Order and Field-Effect Hole Mobility through Control of Nanoscale Polymer Aggregation. *J. Am. Chem. Soc.*

This article is protected by copyright. All rights reserved.

Accepted Manuscript

1864564x, ja, Downloaded from https://chemistry-europe.onlinelibrary.wiley.com/doi/10.1002/cssc.202400171 by Argonne National Laboratory, Wiley Online Library on [25/03/2024]. See the Terms and Conditions (https://onlinelibrary.wiley.com/terms-and-conditions) on Wiley Online Library for rules of use; OA articles are governed by the applicable Creative Commons License

2013, *135* (51), 19229–19236. https://doi.org/10.1021/ja4088665.

(28) Lee, S. M.; Lee, H. R.; Han, A. R.; Lee, J.; Oh, J. H.; Yang, C. High-Performance Furan-Containing Conjugated Polymer for Environmentally Benign Solution Processing. *ACS Appl. Mater. Interfaces* **2017**, *9* (18), 15652–15661. https://doi.org/10.1021/acsami.7b04014.

(29) Wang, Z.; Shi, Y.; Deng, Y.; Han, Y.; Geng, Y. Toward High Mobility Green Solvent-Processable Conjugated Polymers: A Systematic Study on Chalcogen Effect in Poly(Diketopyrrolopyrrole-Alt-Terchalcogenophene)S. *Adv. Funct. Mater.* **2021**, *31* (38), 1–11. https://doi.org/10.1002/adfm.202104881.

(30) Lee, S. M.; Lee, H. R.; Dutta, G. K.; Lee, J.; Oh, J. H.; Yang, C. Furan-Flanked Diketopyrrolopyrrole-Based Chalcogenophene Copolymers with Siloxane Hybrid Side Chains for Organic Field-Effect Transistors. *Polym. Chem.* **2019**, *10* (22), 2854–2862. https://doi.org/10.1039/c9py00448c.

(31) Kang, I.; Yun, H. J.; Chung, D. S.; Kwon, S. K.; Kim, Y. H. Record High Hole Mobility in Polymer Semiconductors via Side-Chain Engineering. *J. Am. Chem. Soc.* **2013**, *135* (40), 14896–14899. https://doi.org/10.1021/ja405112s.

(32) Du, J.; Bulumulla, C.; Mejia, I.; McCandless, G. T.; Biewer, M. C.; Stefan, M. C. Evaluation of (: E)-1,2-Di(Furan-2-Yl)Ethene as Building Unit in Diketopyrrolopyrrole Alternating Copolymers for Transistors. *Polym. Chem.* **2017**, *8* (39), 6181–6187. https://doi.org/10.1039/c7py01373f.

(33) Chen, H.; Guo, Y.; Mao, Z.; Gao, D.; Yu, G. High-Performance Field-Effect Transistors Based on Furan-Containing Diketopyrrolopyrrole Copolymer under a Mild Annealing Temperature. *J. Polym. Sci. Part A Polym. Chem.* **2014**, *52* (14), 1970–1977. https://doi.org/10.1002/pola.27204.

(34) Nielsen, C. B.; Giovannitti, A.; Sbircea, D. T.; Bandiello, E.; Niazi, M. R.; Hanifi, D. A.; Sessolo, M.; Amassian, A.; Malliaras, G. G.; Rivnay, J.; McCulloch, I. Molecular Design of Semiconducting Polymers for High-Performance Organic Electrochemical Transistors. *J. Am. Chem. Soc.* **2016**, *138* (32), 10252–10259. https://doi.org/10.1021/jacs.6b05280.

(35) Chen, S.; Sun, B.; Hong, W.; Aziz, H.; Meng, Y.; Li, Y. Influence of Side Chain Length and Bifurcation Point on the Crystalline Structure and Charge Transport of Diketopyrrolopyrrole-Quaterthiophene Copolymers (PDQTs). *J. Mater. Chem. C* **2014**, *2* (12), 2183–2190. https://doi.org/10.1039/c3tc32219j.

(36) Li, W.; Hendriks, K. H.; Furlan, A.; Roelofs, W. S. C.; Wienk, M. M.; Janssen, R. A. J. Universal Correlation between Fibril Width and Quantum Efficiency in Diketopyrrolopyrrole-Based Polymer Solar Cells. *J. Am. Chem. Soc.* **2013**, *135* (50), 18942–18948. https://doi.org/10.1021/ja4101003.

(37) Li, Y.; Sonar, P.; Singh, S. P.; Zeng, W.; Soh, M. S. 3,6-Di(Furan-2-Yl)Pyrrolo[3,4-c]Pyrrole-1,4(2H,5H)-Dione and Bithiophene Copolymer with Rather Disordered Chain Orientation Showing High Mobility in Organic Thin Film Transistors. *J. Mater. Chem.* **2011**, *21* (29), 10829–10835. https://doi.org/10.1039/c1jm11290b.

(38) Zhong, X.; Chen, T. W.; Yan, L.; You, W. Facile Synthesis of Key Building Blocks of D18 Series Conjugated Polymers for High-Performance Polymer Solar Cells. *ACS Appl. Polym. Mater.* **2023**, *5* (3), 1937–1944. https://doi.org/10.1021/acsapm.2c02009.

(39) Li, W.; Yang, L.; Tumbleston, J. R.; Yan, L.; Ade, H.; You, W. Controlling Molecular Weight of a High Efficiency Donor-Acceptor Conjugated Polymer and Understanding Its Significant Impact on Photovoltaic Properties. *Adv. Mater.* **2014**, *26* (26), 4456–4462.

This article is protected by copyright. All rights reserved.

Accepted Manuscript

1864564x, ja, Downloaded from https://chemistry-europe.onlinelibrary.wiley.com/doi/10.1002/cssc.202400171 by Argonne National Laboratory, Wiley Online Library on [25/03/2024]. See the Terms and Conditions (https://onlinelibrary.wiley.com/terms-and-conditions) on Wiley Online Library for rules of use; OA articles are governed by the applicable Creative Commons License

https://doi.org/10.1002/adma.201305251.

(40) Fu, C.; Bélanger-Gariépy, F.; Perepichka, D. F. Supramolecular Ordering of Difuryldiketopyrrolopyrrole: The Effect of Alkyl Chains and Inter-Ring Twisting. *CrystEngComm* **2016**, *18* (23), 4285–4289. https://doi.org/10.1039/c6ce00383d.

(41) Cao, H.; Rupar, P. A. Recent Advances in Conjugated Furans. *Chem. - A Eur. J.* **2017**, *23* (59), 14670–14675. https://doi.org/10.1002/chem.201703355.

(42) Horner, K. E.; Karadakov, P. B. Chemical Bonding and Aromaticity in Furan, Pyrrole, and Thiophene: A Magnetic Shielding Study. *J. Org. Chem.* **2013**, *78* (16), 8037–8043. https://doi.org/10.1021/jo401319k.

(43) Gidron, O.; Varsano, N.; Shimon, L. J. W.; Leitus, G.; Bendikov, M. Study of a Bifuran vs. Bithiophene Unit for the Rational Design of π-Conjugated Systems. What Have We Learned? *Chem. Commun.* **2013**, *49* (56), 6256–6258. https://doi.org/10.1039/c3cc41795f.

(44) Panzer, F.; Bässler, H.; Köhler, A. Temperature Induced Order-Disorder Transition in Solutions of Conjugated Polymers Probed by Optical Spectroscopy. *J. Phys. Chem. Lett.* **2017**, *8* (1), 114–125. https://doi.org/10.1021/acs.jpclett.6b01641.

(45) Peng, Z.; Ye, L.; Ade, H. Understanding, Quantifying, and Controlling the Molecular Ordering of Semiconducting Polymers: From Novices to Experts and Amorphous to Perfect Crystals. *Mater. Horizons* **2022**, *9* (2), 577–606. https://doi.org/10.1039/d0mh00837k.

(46) Osaka, I.; Takimiya, K. Backbone Orientation in Semiconducting Polymers. *Polymer (Guildf).* **2015**, *59*, A1–A15. https://doi.org/10.1016/j.polymer.2014.12.066.

(47) H. Sirringhaus, P. J. Brown, R. H. Friend, M. M. Nielsen, K. Bechgaard, B. M. W. Langeveld-Voss, A. J. H. Spiering, R. A. J. Janssen, E. W. Meijer, P. H. & D. M. de L. Charge Transport in π-Conjugated Polymers. *Nature* **1999**, *401*, 685–688.

(48) Pandey, M.; Kumari, N.; Nagamatsu, S.; Pandey, S. S. Recent Advances in the Orientation of Conjugated Polymers for Organic Field-Effect Transistors. *J. Mater. Chem. C* **2019**, *7* (43), 13323–13351. https://doi.org/10.1039/c9tc04397g.

(49) Choi, H. H.; Cho, K.; Frisbie, C. D.; Sirringhaus, H.; Podzorov, V. Critical Assessment of Charge Mobility Extraction in FETs. *Nat. Mater.* **2017**, *17* (1), 2–7. https://doi.org/10.1038/nmat5035.

This article is protected by copyright. All rights reserved.

Accepted Manuscript

1864564x, ja, Downloaded from https://chemistry-europe.onlinelibrary.wiley.com/doi/10.1002/cssc.202400171 by Argonne National Laboratory, Wiley Online Library on [25/03/2024]. See the Terms and Conditions (https://onlinelibrary.wiley.com/terms-and-conditions) on Wiley Online Library for rules of use; OA articles are governed by the applicable Creative Commons License